

Figure 5. Stereodiagram illustrating molecular packing of MTX·4H<sub>2</sub>O.

structure (Figure 3a). As noted for the enzyme-bound MTX, these data (Figure 3b) show that strong hydrogen bonds are formed between the  $\alpha$ -carboxylate oxygens with N(1) and N(2); in addition, N(2) forms a second hydrogen bond with an oxygen from the  $\gamma$ -carboxylate. Similarly, N(4) forms weaker hydrogen bonds to the carbonyl oxygens O(17) and O(26). There is also a short intermolecular contact between N(8) and a water molecule, as observed in the enzyme structure.

The conformation of the glutamate moiety and a schematic of the intermolecular contacts for the disordered  $\gamma$ -carboxylate are illustrated in Figure 4. There are four intermolecular hydrogen-bonding contacts to the major conformer [O(26), O(27)] and only one to the minor conformer [O(26'), O(27')] (Table IV). However, two of the contacts to the major conformer have poor hydrogen-bonding geometries; the angles N(2)-H(2)...O(27) and N(4)-H(4)...O(26) are 141.6 and 119.5°, respectively. In addition to the disordered  $\gamma$ -carboxylate, water-3 has at least three possible positions (Table I). Thus, the O(27)...O(W3) contact is only

partially occupied. The short contacts of O(W3) and O(W3'') with O(26') suggest that only O(W3') exists in concert with the minor  $\gamma$ -carboxylate conformer. Water-3 maintains similar contacts to O(25) and O(W1) among its three positions. Since O(W4) lies on a twofold axis, it has two identical contacts with O(W2). One possible intramolecular hydrogen bond exists between N(18) and O(24) with a distance of 2.640 Å.

As shown in the stereopacking diagram (Figure 5), the fourfold symmetry of this crystal structure permits the MTX molecules to pack in such a manner that the  $\alpha$ -carboxylate is in a favorable position to hydrogen bond to the pteridine ring, as observed in the bound enzyme. Also, hydration occurs in clusters along channels between the MTX molecules across the fourfold axis.

The conformational differences observed in MTX structures suggest that it has considerable flexibility, particularly with respect to rotations about the C(6)-C(9) bond. The observation that the specific interactions of the pteridine ring in this determination are analogous to those in the enzyme active site further indicates that this orientation is critical for effective inhibition. The orientation of the benzoylglutamate moiety relative to the pteridine ring is more flexible and can readily accommodate itself to the enzyme requirements. Therefore, several low-energy conformations of MTX are accessible.

In summary, the results of this analysis show that (a) the molecular conformation of MTX is different from that observed in the two bacterial DHFR structures, (b) the intermolecular N...O contacts in the crystal structure are relevant to those found in the enzyme active site environment, and (c) MTX is protonated at N(1). These data also provide reliable details of the hydrogen bond strengths and directionality.

**Acknowledgment.** This research was supported in part by grants from NCI (CA34714) and FRA (287) (V.C.) from the American Cancer Society Faculty Research Award and the Buffalo Foundation. We acknowledge the assistance of Phyllis D. Strong, Dr. Patrick Van Roey, Dr. Walter Pangborn, Elaine De Jarnette, Gloria Del Bel, and Melda Tugac.

## Electrochemical Reductive Activation of Mitomycin C

Paul A. Andrews,\*<sup>1</sup> Su-shu Pan, and Nicholas R. Bachur

Contribution from the The New Frank Bressler Research Laboratories, University of Maryland Cancer Center, Baltimore, Maryland 21201. Received September 20, 1985

**Abstract:** We have used the electrochemical techniques of cyclic voltammetry and preparative flow cell electrolysis to study the role of one-electron vs. two-electron transfer in the reductive activation of mitomycin C (MC) and a primary mitomycin metabolite, 1,2-*cis*-2,7-diamino-1-hydroxymitosene (**6**), to reactive intermediates in polar aprotic solvents. Cyclic voltammetry of MC in DMF (0.1 M TEAP) showed that MC undergoes two quasi-reversible electron-transfer processes at -0.937 and -1.410 V vs. Ag/AgCl, saturated KCl. A following chemical reaction appeared to occur after transfer of a second electron at -1.410 V as indicated by an anodic wave at -0.710 V and a cathodic wave at -0.800 V that appeared upon multicycle scanning. Flow cell reduction at -0.950 V vs. Ag/AgCl, 3 M NaCl over graphite, formed the radical anion of MC in DMF or Me<sub>2</sub>SO as characterized by EPR ( $g = 2.0045$ ). When the radical anion of MC in DMF was mixed with water, parent MC and at least eight other products were generated as detected by HPLC. The one-electron-reduction product profiles showed a pH dependence. Flow cell reduction of MC at -1.450 V formed the dianion of MC in DMF or Me<sub>2</sub>SO, which generated only two products when mixed with water. These products have been identified by mass spectral and NMR analyses to be 10-decarbonyl-2,7-diaminomitosene (**14**) and 2,7-diamino-2,3-dihydro-6-methyl-1*H*-pyrrolo[1,2-*a*]indole-5,8-dione (**22**). Generation of **22** was completely suppressed when the dianion was added to phosphate buffer. Flow cell reduction of **6** in DMF at -1.200 or -1.500 V generated the radical anion ( $g = 2.0045$ ) or dianion, respectively. These species both gave 1,2-*cis*-2,7-diamino-2,3-dihydro-6,9-dimethyl-1-hydroxy-1*H*-pyrrolo[1,2-*a*]indole-5,8-dione (**27**) as the sole product when mixed with water. These data provide evidence that one-electron reduction is sufficient to activate MC and its primary metabolites to reactive intermediates. Furthermore, the results suggest that one-electron transfer is the dominant mode of bioreductive activation since the HPLC profile of the radical-anion-generated products of MC closely resembled the profile of metabolites generated from reduction with purified flavoenzymes.

Mitomycin C (MC; **1**) is a quinone-containing antitumor antibiotic that alkylates DNA, RNA, and protein;<sup>2</sup> cross-links

complimentary DNA strands;<sup>3-5</sup> and cross-links DNA with protein.<sup>3,5</sup> The covalent attachment of MC to DNA is believed to

account for the drug's anticancer activity. Although the exact nature of the interstrand cross-links induced in DNA by MC remains unknown, the chemical structure of the monoadducts of MC with DNA have recently been reported.<sup>6-8</sup> The intracellular expression of MC's alkylating ability is, however, contingent upon the reduction of the quinone moiety by native enzymes.<sup>9-11</sup> In particular, the flavoproteins NADPH cytochrome P-450 reductase (EC 1.6.2.4) and xanthine oxidase (EC 1.2.3.2) appear to be the dominant intracellular reductive catalysts.<sup>12-14</sup> Due to this activation requirement for cytotoxicity, MC has been termed the prototypical bioreductive alkylating agent<sup>15-17</sup> and has served as a model that has spawned the synthesis of innumerable compounds designed to possess antineoplastic activity following bioreductive activation.<sup>16</sup>

Despite the clear need for bioreduction in this class of drugs, the role of one-electron vs. two-electron reduction of the quinone moiety in the expression of MC's alkylating properties is an enigma. Most of the proposed mechanisms for the cross-linking reactions and metabolic transformations of MC have assumed an initial two-electron reduction of the drug to the hydroquinone.<sup>10,11,16-18</sup> Various pathways have been conjectured, which then lead from the hydroquinone to a bifunctionally reactive, quinone methide intermediate by loss of methanol between C-9 and C-9a, opening of the aziridine at C-1, and loss of the carbamoyl group at C-10. Studies on the enzymatically generated one-electron-reduced MC semiquinone, or radical anion, have focused not on its propensity to decompose to an alkylating intermediate but on the ability of this species to transfer an electron to molecular oxygen to generate superoxide<sup>19-21</sup> and parent drug. Superoxide and other reactive oxygen species have also been postulated to arise from sequential oxidation of the purported hydroquinone,<sup>18,22</sup> and it is these secondary reactive oxygen species that are believed to cause the DNA strand cleavage seen in cells treated with MC. With regard to the role of the one-electron-reduced species in eliciting the alkylating ability of MC, a single report by Tomasz et al.,<sup>23</sup> in which sodium dithionite reduction

was used as a model for bioreduction, has suggested that the primary reactive species for DNA binding was the radical anion of MC.

To better define the role of one-electron vs. two-electron reduction of MC in its metabolism and transformation to an alkylating intermediate, we utilized electrochemical methods to model the reductive activation of MC by the flavoenzymes xanthine oxidase and NADPH cytochrome P-450 reductase. By carefully controlling the reduction potential in the polar aprotic solvents DMF and Me<sub>2</sub>SO, in which the reduction of a quinone exhibits two clearly separable one-electron steps,<sup>24</sup> we were able to produce distinct, concentrated solutions of either the one-electron-reduced radical anion or the two-electron-reduced dianion of MC. The reduced species of a primary 1,2-*cis*-mitosene metabolite, **6**, were also produced in this manner. This approach allowed the spectroscopic study of these species by absorbance and EPR spectrometry and the subsequent characterization of decomposition products of each species following reaction with water under anaerobic conditions. The results clearly show that one-electron reduction is sufficient to generate an activated intermediate of both MC and a primary metabolite, **6**.

### Experimental Section

**Materials.** Mitomycin C was obtained from Bristol Laboratories, Syracuse, NY and was 99% pure as determined by HPLC. Polarography grade tetraethylammonium perchlorate (TEAP) was from Kodak (Rochester, NY). HPLC grade dimethylformamide (DMF) was from Burdick and Jackson Laboratories (Muskegon, MI) and was stored over molecular sieves. Spectrophotometric grade dimethyl sulfoxide (Me<sub>2</sub>SO) was from Aldrich Chemical Co. (Milwaukee, WI). *cis*-2,7-Diamino-1-hydroxymitosene (**6**) was synthesized from MC and separated from the trans isomer (**7**) by semipreparative HPLC.<sup>25</sup> 10-Decarbamoyl-mitomycin C (**11**) was prepared as described.<sup>26</sup>

**Electrochemistry.** Cyclic voltammetry was performed with a CV-IA voltammetry unit (Bioanalytical Systems, West Lafayette, IN) connected to a thermostated electrochemical cell (IBM Instruments Inc., Danbury, CT). All voltammograms were obtained with the cell maintained at 25 °C by a Lauda B-1 circulating water bath (MGW Lauda). The platinum wire counter electrode, platinum working electrode (0.159 cm<sup>2</sup>), and Ag/AgCl (saturated KCl) reference electrode were all obtained from IBM Instruments. Solutions were sparged with nitrogen 10 min prior to scanning and maintained under a nitrogen atmosphere during scanning. Reported potentials were taken from the first cycle. Rates of electron transfer were calculated according to Bard and Faulkner.<sup>27</sup>

For preparative generation of reduced MC and **6** species, an electrochemical flow cell was constructed (Consolidated Instruments Corp., Baltimore, MD) similar to a literature design<sup>28</sup> and is described fully in the supplementary material. The calibration and operating characteristics of this flow cell have been previously described.<sup>29</sup> Anaerobic reductions were done with the equipment in a nitrogen-purged glovebox maintained with a positive nitrogen atmosphere. Reduced solutions were collected either in stoppered quartz cuvettes directly for EPR and absorbance analysis or in deaerated water or deaerated 0.1 M phosphate buffer.

**Spectroscopic Methods.** A Varian X-band (9.3 GHz) E-109 electron paramagnetic resonance (EPR) spectrometer fitted with a dual rectangular cavity (TM-104) was used to detect and characterize free-radical species. The modulation frequency was 100 kHz. Solutions of free-radical species were transferred to standard EPR aqueous flat cells in the nitrogen-purged glovebox. Spectra were recorded with a cavity temperature of 20 °C. *g* values were calculated against standard pitch (*g* = 2.0028) placed in the rear cavity.

Electron ionization mass spectra were obtained with a direct-inlet probe on a VG 30F mass spectrometer (VG Analytical, Altrincham, Great Britain) operated under VG Data Systems 2040 computer control. Source conditions were 200 °C, 70 eV, 170-μA trap current, and 4-kV

- (1) Present address: Cancer Center, UCSD T-012, La Jolla, CA 92093.
- (2) Weissbach, A.; Lisio, A. *Biochemistry* **1965**, *4*, 196-200.
- (3) Dorr, R. T.; Bowden, G. T.; Alberts, D. S.; Liddil, J. D. *Cancer Res.* **1985**, *45*, 3510-3516.
- (4) Iyer, V. N.; Szybalski, W. *Proc. Natl. Acad. Sci. U.S.A.* **1963**, *50*, 355-362.
- (5) Meyn, R. E.; Jenkins, S. F.; Thompson, L. H. *Cancer Res.* **1982**, *42*, 3106-3110.
- (6) Hashimoto, Y.; Shudo, K.; Okamoto, T. *Chem. Pharm. Bull.* **1983**, *31*, 861-869.
- (7) Tomasz, M.; Lipman, R.; Snyder, J. K.; Nakanishi, K. *J. Am. Chem. Soc.* **1983**, *105*, 2059-2063.
- (8) Pan, S.; Iracki, T.; Bachur, N. R. *Mol. Pharmacol.*, 1986, in press.
- (9) Schwartz, H. S.; Sodergren, J. E.; Phillips, F. S. *Science (Washington, D.C.)* **1963**, *142*, 1181-1183.
- (10) Iyer, V. N.; Szybalski, W. *Science (Washington, D.C.)* **1964**, *145*, 55-58.
- (11) Tomasz, M.; Lipman, R. *Biochemistry* **1981**, *20*, 5056-5061.
- (12) Pan, S.; Andrews, P. A.; Glover, C. J.; Bachur, N. R. *J. Biol. Chem.* **1984**, *259*, 959-966.
- (13) Komiyama, T.; Oki, T.; Inui, T. *J. Pharmacobio-Dyn.* **1979**, *2*, 407-410.
- (14) Keyes, S. R.; Fracasso, P. M.; Heimbrook, D. C.; Rockwell, S.; Sligar, S. G.; Sartorelli, A. C. *Cancer Res.* **1984**, *44*, 5638-5643.
- (15) Lin, A. J.; Cosby, L. A.; Sartorelli, A. C. *ACS Symp. Ser.* **1976**, No. 30, 71-86.
- (16) Moore, H. W. *Science (Washington, D.C.)* **1977**, *197*, 527-532.
- (17) Lin, A. J.; Cosby, L. A.; Shansky, C. W.; Sartorelli, A. C. *J. Med. Chem.* **1972**, *15*, 1247-1252.
- (18) Lown, J. W. In *Mitomycin C—Current Status and New Developments*; Carter, S. K., Crooke, S. T., Eds.; Academic: New York, 1979; pp 5-26.
- (19) Bachur, N. R.; Gordon, S. L.; Gee, M. V.; Kon, H. *Proc. Natl. Acad. Sci. U.S.A.* **1979**, *76*, 954-957.
- (20) Doroshov, J. H. *J. Pharmacol. Exp. Ther.* **1981**, *218*, 206-211.
- (21) Hando, K.; Sato, S. *Gann* **1975**, *66*, 43-47.
- (22) Tomasz, M. *Chem.-Biol. Interact.* **1976**, *13*, 89-97.
- (23) Tomasz, M.; Mercado, C. M.; Olson, J.; Chatterjee, N. *Biochemistry* **1974**, *13*, 4878-4887.

(24) Chambers, J. Q. In *The Chemistry of the Quinoid Compounds*, Part 2; Patai, S., Ed.; Wiley: New York, 1974.

(25) Andrews, P. A.; Pan, S.; Bachur, N. R. *J. Chromatogr.* **1983**, *262*, 231-247.

(26) Kinoshita, S.; Uzu, K.; Nakano, K.; Takahashi, T. *J. Med. Chem.* **1971**, *14*, 109-112.

(27) Bard, A. J.; Faulkner, L. R. *Electrochemical Methods*; Wiley: New York, 1980; pp 230-231.

(28) Miner, D. J.; Kissinger, P. T. *Biochem. Pharmacol.* **1979**, *28*, 3285-3290.

(29) Andrews, P. A. Ph.D. Dissertation, University of Maryland at Baltimore, 1983.

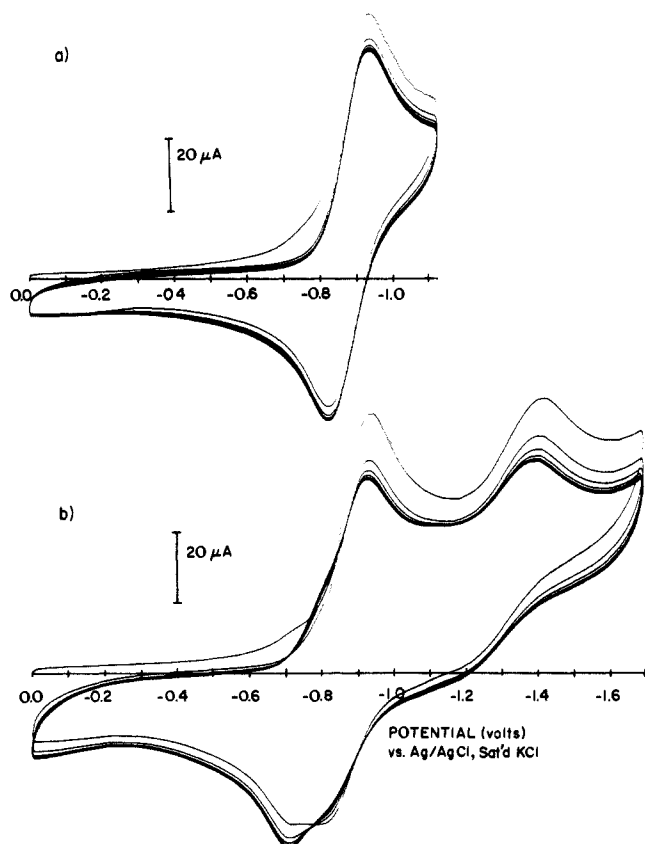


**Figure 1.** Multicycle cyclic voltammograms of 0.83 mM MC in DMF (0.1 M TEAP) at  $500 \text{ mV s}^{-1}$  in the potential range (a) 0.0 to  $-1.125 \text{ V}$  and (b) 0.0 to  $-1.700 \text{ V}$  vs. Ag/AgCl, saturated KCl.

accelerating voltage. Mass spectra of acetylated compounds were obtained on a Vespel rod probe tip as previously described.<sup>25</sup>

The proton NMR spectra were obtained on a Nicolet NT 360-MHz NMR spectrometer (Fremont, CA) or on a JEOL FX 60-MHz NMR spectrometer both operated in the FT mode and provided by Dr. Robert J. Hight of the National Heart, Lung, and Blood Institute, NIH, Bethesda, MD. Spectra were obtained in  $\text{CD}_3\text{OD}$ , and chemical shifts are relative to tetramethylsilane.

UV-visible absorption spectra were recorded on a Beckman Acta IIIC spectrophotometer (Beckman Instruments, Inc., Fullerton, CA). MC and **6** concentrations were determined, respectively, at 365 (molar absorptivity 21 400) and 313 nm (molar absorptivity 11 400).

**Chromatography.** Analytical and semipreparative HPLC was performed as previously described.<sup>25</sup> Briefly, for analytical separations, compounds were eluted from a 10-cm  $\times$  8.0-mm Radial-PAK  $\text{C}_{18}$  cartridge (10- $\mu\text{m}$  particle size) (Waters Associates) with a linear 13-min gradient from 0 to 50% methanol in 0.01 M, pH 7.0 potassium phosphate buffer. The flow rate was 3.0 mL/min, and compounds were detected at 365, 313, or 280 nm. SEP-PAK  $\text{C}_{18}$  cartridges (Waters Associates) were used for desalting and concentrating collected peaks for subsequent structural analysis.

## Results

**Electrochemistry.** The cyclic voltammetric analysis of 0.83 mM MC in DMF (0.1 M TEAP) at a platinum electrode in the potential range 0.000 to  $-1.125 \text{ V}$  at a sweep rate ( $\nu$ ) of  $500 \text{ mV s}^{-1}$  gave a single cathodic wave at  $-0.937 \text{ V}$  and a single anodic wave at  $-0.825 \text{ V}$  vs. Ag/AgCl, saturated KCl (Figure 1a). The shift of the cathodic peak to  $-0.925 \text{ V}$  at  $50 \text{ mV s}^{-1}$  and the shift in the difference in peak potentials ( $\Delta E_p$ ) from 112 mV at  $500 \text{ mV s}^{-1}$  to 80 mV at  $50 \text{ mV s}^{-1}$  indicated that this was a quasi-reversible charge-transfer process. The plot of the peak current ( $i_p$ ), however, increased linearly with  $\nu^{1/2}$  between 50 and  $500 \text{ mV s}^{-1}$ , indicative of a diffusion-controlled charge-transfer process. When the slope in this linear portion of the plot and the Randles-Sevcik equation were used, a diffusion coefficient of  $8.3 \times 10^{-6} \text{ cm}^2 \text{ s}^{-1}$  was calculated in good agreement with values determined in DMF for other quinone-containing antibiotics of similar molecular weight.<sup>29</sup> The constancy of the anodic and

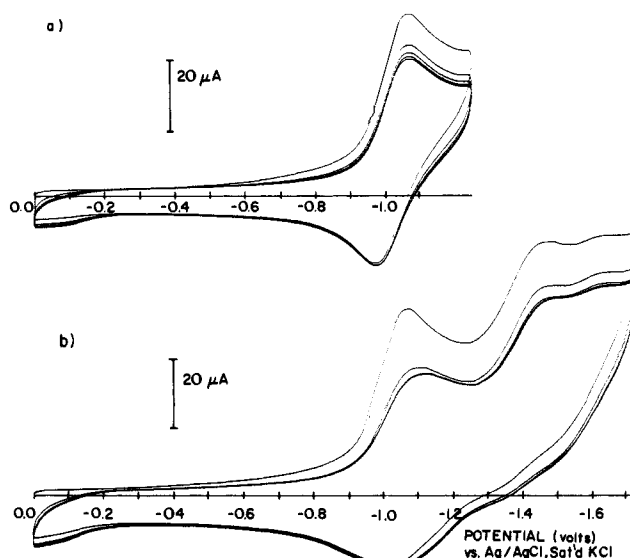


**Figure 2.** Multicycle cyclic voltammograms of 0.63 mM **6** in DMF (0.1 M TEAP) at  $500 \text{ mV s}^{-1}$  in the potential range (a) 0.0 to  $-1.250 \text{ V}$  and (b) 0.0 to  $-1.740 \text{ V}$  vs. Ag/AgCl, saturated KCl.

cathodic peak currents with multicycle sweeps reflected the stability of the charge-transfer product, the MC radical anion, in an aprotic solvent. The heterogeneous rate constant ( $k^0$ ) for electron transfer from the electrode to MC was estimated to be  $9.8 \times 10^{-3} \text{ cm s}^{-1}$ .

When the switching potential was changed to  $-1.700 \text{ V}$ , a more complex voltammogram was obtained (Figure 1b). As expected, a second cathodic wave appeared at  $-1.410 \text{ V}$  ( $500 \text{ mV s}^{-1}$ ), corresponding to the transfer of an electron to the MC radical anion to generate the MC dianion. This wave shifted to  $-1.395 \text{ V}$  at  $\nu = 50 \text{ mV s}^{-1}$ , indicating that this charge-transfer process was also quasi-reversible. On the anodic sweep, a poorly defined wave appeared at  $-1.200 \text{ V}$ , which was barely discernible at slow sweep rates ( $50 \text{ mV s}^{-1}$ ) and which is due to reoxidation of the MC dianion. Anodic waves also occurred at  $-0.805$  and  $-0.710 \text{ V}$ . With repetitive scanning, the peak current of the  $-0.805\text{-V}$  wave, corresponding to oxidation of the MC radical anion, diminished so that the wave appeared as a shoulder, and the  $-0.710\text{-V}$  peak current increased. With multicycle scanning, a shoulder also appeared on the cathodic scan at  $-0.800 \text{ V}$ , which grew more prominent with scan number.

Similar results were obtained when the cyclic voltammograms of MC were taken in  $\text{Me}_2\text{SO}$  (0.1 M TEAP) (data not shown). The cathodic waves occurred at  $-0.905$  and  $-1.545 \text{ V}$ . Anodic waves occurred at  $-1.220$ ,  $-0.820$  (sh), and  $-0.695 \text{ V}$ . The diffusion coefficient was  $2.3 \times 10^{-6} \text{ cm}^2 \text{ s}^{-1}$ , in line with the higher viscosity of  $\text{Me}_2\text{SO}$  compared to DMF.<sup>30</sup> The  $k^0$  was estimated to be  $11.4 \times 10^{-3} \text{ cm s}^{-1}$ .

Cyclic voltammetric analysis of **6** (0.63 mM) in DMF (0.1 M TEAP) with a switching potential of  $-1.250 \text{ V}$  and  $\nu = 500 \text{ mV s}^{-1}$  gave a cathodic wave at  $-1.070 \text{ V}$  and an anodic wave at  $-0.975 \text{ V}$  (Figure 2a). At  $50 \text{ mV s}^{-1}$  these shifted to  $-1.055$  and  $-0.995 \text{ V}$  as the  $\Delta E_p$  shifted from 95 to 60 mV, indicating quasi-reversible charge transfer. The peak current was linear with  $\nu^{1/2}$  over this scan range, however, and the diffusion coefficient was  $7.4 \times 10^{-6} \text{ cm}^2 \text{ s}^{-1}$ . The  $k^0$  was estimated to be  $15.6 \times 10^{-3} \text{ cm s}^{-1}$ . Multicycle sweeps showed that the **6** radical anion was stable. When the switching potential was changed to  $-1.740 \text{ V}$ , cathodic waves appeared at  $-1.463$  and  $-1.630 \text{ V}$  ( $500 \text{ mV s}^{-1}$ ) (Figure 2b). At  $50 \text{ mV s}^{-1}$ , the  $-1.463\text{-V}$  wave, attributed to generation of **6** dianion, moved to  $-1.440 \text{ V}$ . The  $-1.630\text{-V}$  wave did not move at slower sweep rates; however, exact determination of  $E_p$  was difficult due to the broadness of the peak. On the anodic sweep, two shoulders were discernible at  $-1.495$  and  $-1.355 \text{ V}$  and a broad

(30) Stokes, R. H.; Mills, R. *Viscosity of Electrolytes and Related Properties*; Pergamon: New York, 1965; p 76.

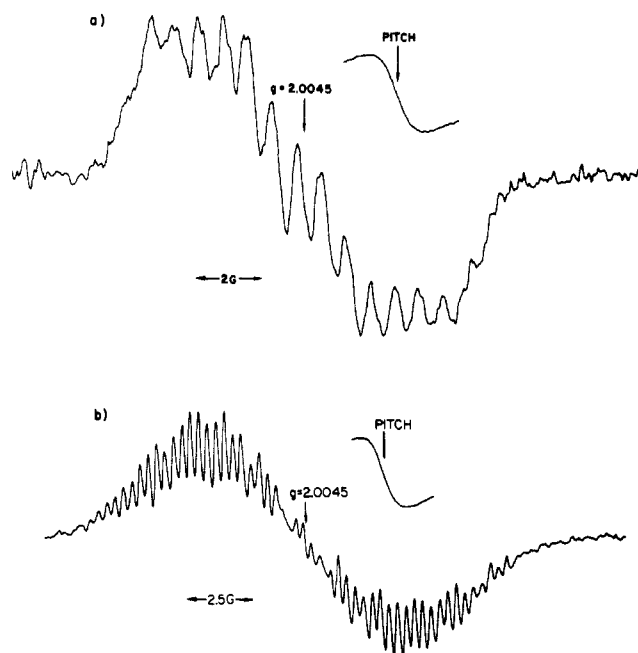


**Figure 3.** EPR analysis of (a) the MC radical anion and (b) the 6 radical anion recorded in DMF (0.1 M TEAP). Scan conditions: (a) 2.5 G/min, 1-s time constant, 0.5-G modulation amplitude, 10-mW incident microwave power,  $1.25 \times 10^4 \times 10$  gain; (b) 6.25 G/min, 0.5-s time constant, 0.1-G modulation amplitude, 10-mW incident microwave power,  $5 \times 10^3 \times 10$  gain.

wave at  $-1.008$  V corresponding to oxidation of the radical anion to 6. No new cathodic waves appeared with multicycle scanning.

**Decomposition of the MC Radical Anion and Dianion in  $H_2O$ .** Reduction of 1.44 mM MC in DMF (0.1 M TEAP) at  $-0.950$  V vs. Ag/AgCl, 3 M NaCl, in the electrochemical flow cell produced a light brown solution with absorbance maxima at 316 and 370 nm. EPR analysis of this anaerobic solution gave an intense multilined spectrum at  $g = 2.0045$  (spectrum width 12.5 G), verifying the presence of the MC radical anion (Figure 3a). Exposure of this solution to air regenerated an absorbance spectrum similar to that of MC ( $\lambda_{max} = 366$  nm) with a shoulder at 312 nm. Direct collection of 0.5 mL of the anaerobic solution in 1.0 mL of deaerated water caused an immediate change in color to bright purple. HPLC analysis of the resultant solution gave a profile of nine major products (Figure 4a). The profile was independent of the time after mixing that the solution was analyzed. Some of these peaks were tentatively identified by co-chromatography with known standards<sup>25</sup> as follows. MC, with higher absorbance at 365 nm than at 313 nm, was eluted at  $k' = 12.0$  ( $t_0 = 0.7$ ). 10-Decarbamoyl-MC (11), also with higher absorbance at 365 nm, was eluted at  $k' = 11.4$ . 7 was eluted at  $k' = 10.7$ . The peak just in front of this compound was attributed to 13.<sup>25</sup> The peak that was eluted just after MC at  $k' = 12.6$  was unidentified; however, the only other compound we have ever observed in this region of the chromatogram is  $N^2$ -formyl-6, which arose during the acid hydrolysis of MC with DMF present.<sup>25</sup> This compound may possibly be formed following reduction of MC with high concentrations (33%) of DMF present, although this peak was also observed in reductions carried out in  $Me_2SO$ . The  $k' = 13.9$  peak was assigned to 6 and the shoulder on its front side to 12. The  $k' = 14.9$  peak cochromatographed with a peak generated from two-electron reduction of MC (14; see below). The  $k' = 15.6$  peak was identified as 8. When the DMF/ $H_2O$  ratio was reversed (1.0 mL was collected in 0.5 mL of water), no change in the products or their ratios was observed (data not shown).

One-electron reduction of MC in  $Me_2SO$  also gave a solution with a multilined EPR spectrum at  $g = 2.0045$  (data not shown). HPLC analysis of 0.5 mL of this solution mixed with 1.0 mL of  $H_2O$  gave multiple products in a poorly resolved chromatogram (supplementary material). Three products were tentatively

**Table I.**  $^1H$  NMR Data<sup>a</sup> for Two-Electron-Reduction Products of MC and 6

MC		6
$k' = 14.9^b$ (14)	$k' = 17.1^c$ (22)	$k' = 16.5^c$ (27)
1.78 (s, 3 H, $C_6$ CH <sub>3</sub> )	1.80 (s, 3 H, $C_6$ CH <sub>3</sub> )	1.74 (s, 3 H, $C_6$ CH <sub>3</sub> )
2.14 (m, $C_1$ H <sub><math>\beta</math>)</sub>	2.61 (dd, 1 H, $J = 16, 4.5$ Hz, $C_1$ H <sub><math>\beta</math>)<sup>d</sup></sub>	2.24 (s, 3 H, $C_9$ CH <sub>3</sub> )
2.73 (m, $C_1$ H <sub><math>\alpha</math>)</sub>	3.13 (m, 1 H, $C_1$ H <sub><math>\alpha</math>)</sub>	3.58 (dd, 1 H, $J = 12, 8$ Hz, $C_3$ H <sub><math>\beta</math>)</sub>
3.5–4.5 (m, $C_2$ H, $C_3$ H <sub>2</sub> )	3.95 (dd, 1 H, $J = 12.5, 4.5$ Hz, $C_3$ H <sub><math>\beta</math>)</sub>	3.78 (m, 1 H, $C_2$ H)
4.66 (s, 2 H, $C_{10}$ H <sub>2</sub> ) <sup>e</sup>	4.19 (m, 1 H, $C_2$ H)	4.31 (dd, 1 H, $J = 12.4, 7.6$ Hz, $C_3$ H <sub><math>\alpha</math>)</sub>
	4.39 (dd, 1 H, $J = 12.5, 6.5$ Hz, $C_3$ H <sub><math>\alpha</math>)</sub>	4.59 (d, 1 H, $J = 6$ Hz, $C_1$ H <sub><math>\alpha</math>)</sub>
	6.18 (s, 1 H, $C_9$ H)	6.47 (s, 2 H, $C_7$ NH <sub>2</sub> )

<sup>a</sup> In  $\delta$  relative to  $Me_4Si$ . Spectra were obtained in  $CD_3OD$ . <sup>b</sup> 60 MHz. <sup>c</sup> 360 MHz. <sup>d</sup> Assignments assume  $\alpha$ -hydrogens appear downfield from  $\beta$ -hydrogens<sup>33</sup> in light of the recent reassignment of the structure of MC.<sup>34</sup> <sup>e</sup> Literature value<sup>6</sup> for 10-decarbomoyl-2,7-diaminomitosene in  $Me_2SO-d_6$  is  $\delta$  4.72.

identified as follows: 7,  $k' = 10.7$ ; MC,  $k' = 12.0$ ; 6,  $k' = 13.9$ .

Reduction of 1.44 mM MC in DMF at  $-1.450$  V in the flow cell also generated a light brown solution with absorbance maxima at 324 and 379 nm. Collection of 0.5 mL of this solution in 1.0 mL of deaerated water caused an immediate color change to bright purple as occurred with the  $-0.950$ -V reduction solution. HPLC of this solution gave a profile of only two major peaks at  $k' = 14.9$  and 17.1 (Figure 4b). Identification of these peaks as 14 and 22 will be described below. No change in the results was observed when 1 mL of solution was collected in 0.5 mL of water. Reduction of MC in  $Me_2SO$  at  $-1.450$  V gave identical data.

**Decomposition of 6 in  $H_2O$ .** A solution of 1.4 mM 6 in DMF (0.1 M TEAP) was reduced at either  $-1.200$  or  $-1.500$  V. EPR analysis of the  $-1.200$ -V-reduced solution gave an intense 53-line spectrum at  $g = 2.0045$  (17.5-G spectrum width), which verified the presence of the 6 radical anion (Figure 3b). The species resulting from reduction at  $-1.200$  and  $-1.500$  V were separately mixed (0.5 mL) with 1.0 mL of deaerated water. HPLC analysis of both of these solutions gave a single peak at  $k' = 16.5$  (Figure 4c). Identification of this product as 27 will be described below.

**Identification of Two-Electron-Reduction Products of MC.** The two major products obtained from reaction of the MC dianion with  $H_2O$  were separated by semipreparative HPLC. The absorbance spectra of the  $k' = 14.9$  and 17.1 products (14, 22) in methanol had maxima at 314 nm indicative of mitosene compounds. The EI mass spectrum of the  $k' = 14.9$  product gave a strong molecular ion at  $m/z$  261 ( $M^+$ ). After acetylation, this compound had a  $k' = 18.4$ , and the mass spectrum of this product suggested that two acetyl groups had been added. The fragmentation was consistent with the proposed structure.<sup>25,31</sup> The absence of an intense fragment ion at  $m/z$  44 (carbamylium ion,  $CONH_2^+$ ) in either spectrum indicated that the carbamoyl group was not present.<sup>25</sup> NMR analysis indicated a singlet at  $\delta$  4.66 (2 H) that was assigned to  $C_{10}$  (Table I).<sup>32</sup> To corroborate our structural assignment of the  $k' = 14.9$  peak as 10-decarbomoyl-2,7-diaminomitosene (14), we synthesized this compound unambiguously by catalytic hydrogenation of 11.<sup>11</sup> The major product from this reaction cochromatographed with the electrochemical product and had an identical EI mass spectrum (supplementary material), thus confirming the identity of this compound.

The EI mass spectrum of the  $k' = 17.1$  product gave a molecular ion at  $m/z$  231 ( $M^+$ ). The mass spectrum of the acetylated

(31) Since only low-resolution mass spectra were obtained, the proposed fragmentations are tentative.

(32) Literature values for the chemical shift of the  $C_{10}$  protons when the carbamoyl group is present range from  $\delta$  4.91 to 5.25.

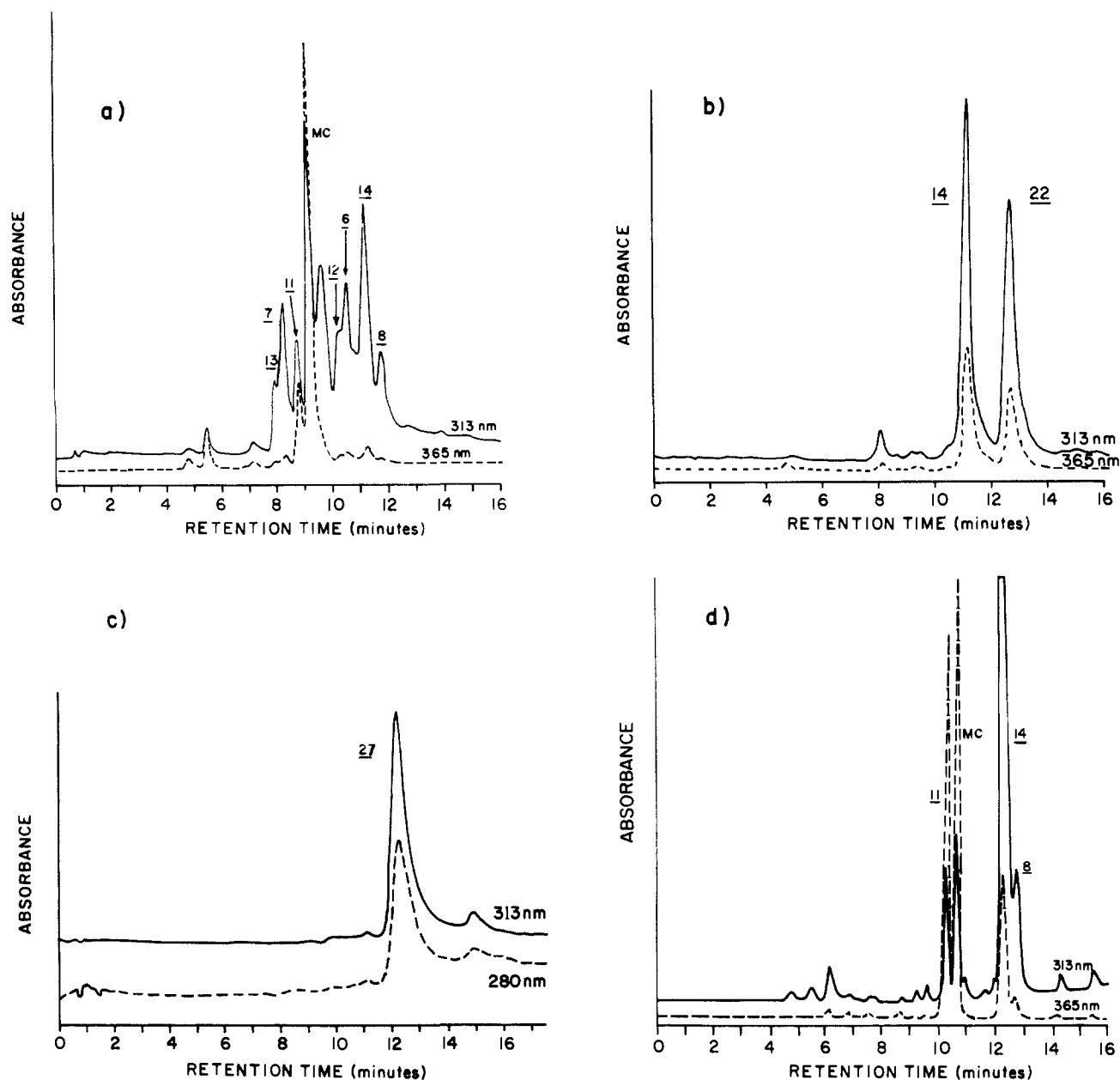


**Figure 4.** HPLC profiles of the products generated from the radical anions and dianions of MC or 6 reacting with water:<sup>35</sup> (a) 0.5 mL of the MC radical anion, (b) 0.5 mL of the MC dianion, and (c) 0.5 mL of the 6 radical anion or dianion in DMF (0.1 M TEAP) after mixing anaerobically with 1.0 mL of water; (d) 0.5 mL of the MC radical anion mixed anaerobically with 0.1 M potassium phosphate buffer, pH 7.1.

product, now with  $k' = 15.9$ , showed the addition of one acetyl group. The carbamoyl group was absent. The high-resolution NMR spectrum of the  $k' = 17.1$  product (Table I) indicated that the C-1 position was unsubstituted<sup>11,33</sup> [ $\delta$  2.61 (1 H, C<sub>1</sub> H <sub>$\alpha$</sub> ),  $\delta$  3.13 (1 H, C<sub>1</sub> H <sub>$\beta$</sub> )]. A singlet at  $\delta$  6.18 (1 H) indicated a single olefinic proton that was assigned to C-9. The structure of this compound was thus deduced as the novel mitosene 2,7-diamino-2,3-dihydro-6-methyl-1*H*-pyrrolo[1,2-*a*]indole-5,8-dione (22).

**Identification of the Reduction Product of 6.** The reaction of both the radical anion and the dianion of 6 with H<sub>2</sub>O gave an identical solitary product at  $k' = 16.5$  by HPLC. The absorbance spectrum in methanol had a maximum at 314 nm, indicative of the mitosene chromophore. The EI mass spectrum of this product was similar to the mass spectrum of 14 in that most of the major fragment ions were the same, yet their relative intensities were markedly and reproducibly different. The addition of two acetyl groups upon acetylation of this product, now at  $k' = 19.2$ , indicated the presence of two labile protons. The carbamoyl group was

absent as indicated by low intensity at  $m/z$  44. The high-resolution NMR of this product (Table I) showed that a hydroxy substituent remained at C-1 [ $\delta$  4.59 (1 H, C<sub>1</sub> H <sub>$\alpha$</sub> )].<sup>11,33</sup> A singlet at  $\delta$  2.24 (3 H) was assigned to a methyl group at C-9. The structure of the one- or two-electron-reduction product of 6 was thus deduced as 1,2-*cis*-2,7-diamino-2,3-dihydro-6,9-dimethyl-1-hydroxy-1*H*-pyrrolo[1,2-*a*]indole-5,8-dione (27).

**Buffer and pH Effects.** Phosphate buffer and its pH had several effects on the products obtained upon mixing the reduced MC and 6 species with H<sub>2</sub>O. Unlike enzymatic reduction,<sup>11,12</sup> no peaks corresponding to the 1-phosphomitosenes were generated from any of these species with phosphate buffer. The phosphate buffer did, however, effect the relative profile of products seen by HPLC. When the radical anion of MC was mixed with pH 7.1, 0.1 M potassium phosphate buffer instead of H<sub>2</sub>O, the relative yield of MC, 11, 14, and 8 increased as the 6, 7, 12, 13, and  $k' = 12.6$  peaks diminished in yield (Figure 4d).<sup>35</sup> Similar changes in the

(33) Kohn, H.; Zein, N. *J. Am. Chem. Soc.* **1983**, *105*, 4105-4106.

(34) Shirahata, K.; Hirayama, N. *J. Am. Chem. Soc.* **1983**, *105*, 7199-7200.

(35) The chromatograms in Figure 4 cannot be compared directly as these were taken from different experiments that used different Radial-PAK cartridges and slightly different concentrations of MC. The capacity factors and selectivities of these compounds vary from cartridge to cartridge.

Scheme I

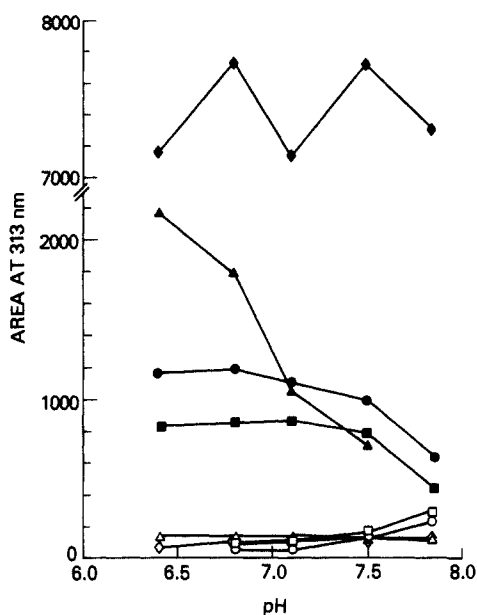
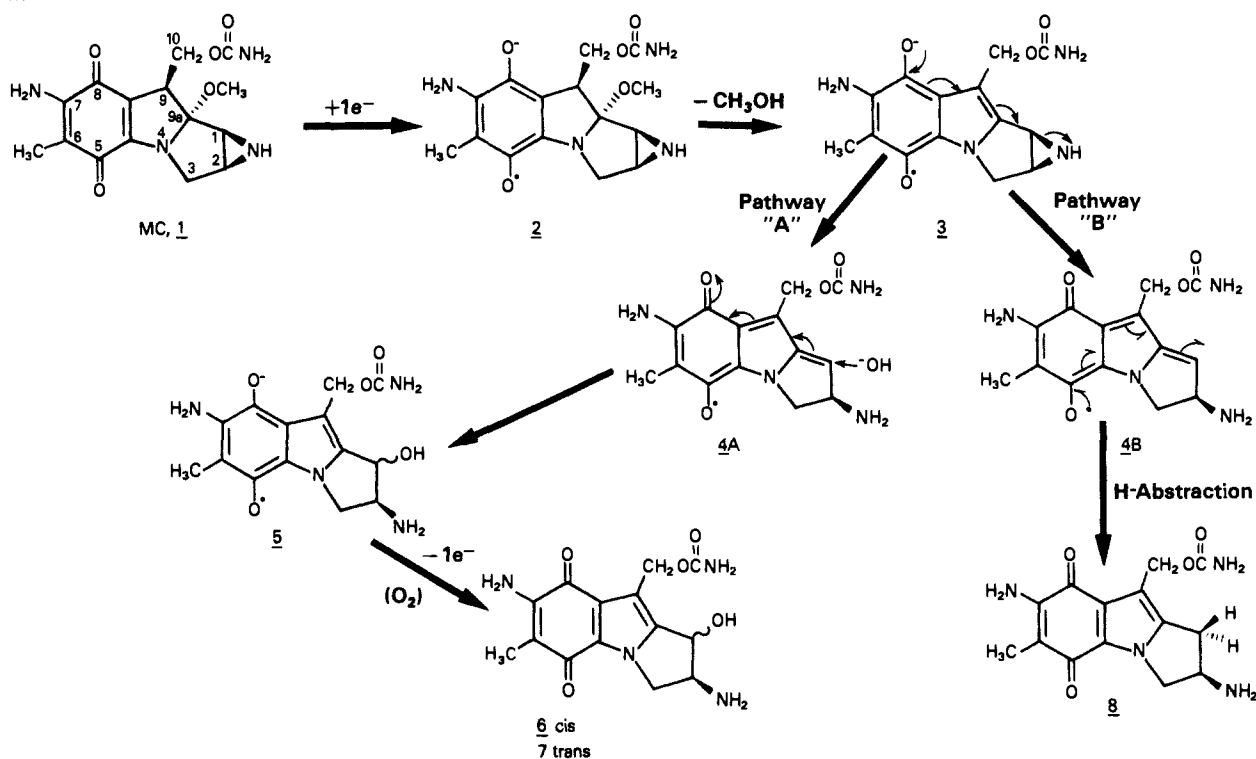
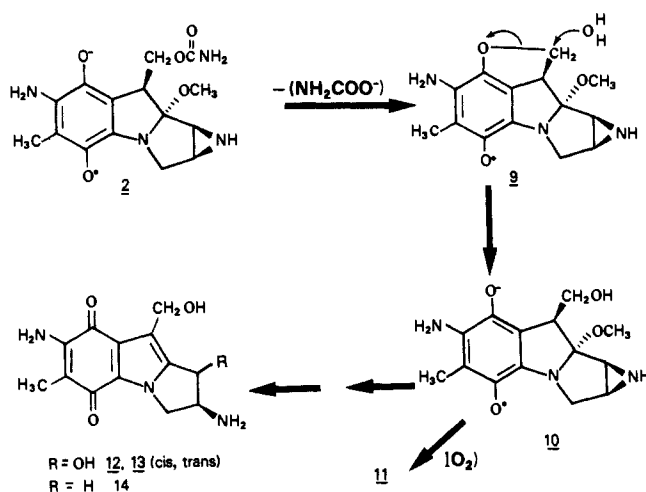


**Figure 5.** pH effect on the product profile generated from the MC radical anion mixed with phosphate buffer. Products were generated by adding 0.5 mL of MC radical anion in DMF (0.1 M TEAP) to 1 mL of deaerated potassium phosphate buffer: ●, MC; ■, 11; ▲, 8; ◆, 14; □, 6; ◇, 7; ○, 12; △, 13.

product profile were seen when the radical anion in Me<sub>2</sub>SO was added to pH 7.5, 0.2 M phosphate buffer (supplementary material). The pH of the buffer also affected the product profile. Analogous to the enzymatic reduction of MC,<sup>11,12</sup> the amount of 8 generated from MC radical anion increased with acidic pH (Figure 5), and the 1-hydroxymitosenes (6, 7, 12, 13) decreased in relative amount as the pH decreased.

Interestingly, when the MC dianion was mixed with phosphate buffer instead of H<sub>2</sub>O, the phosphate completely suppressed the formation of 22 such that 14 was the sole product at all pHs (data not shown). The phosphate buffer had no effect on the generation of 27 from either the 6 radical anion or dianion.

Scheme II

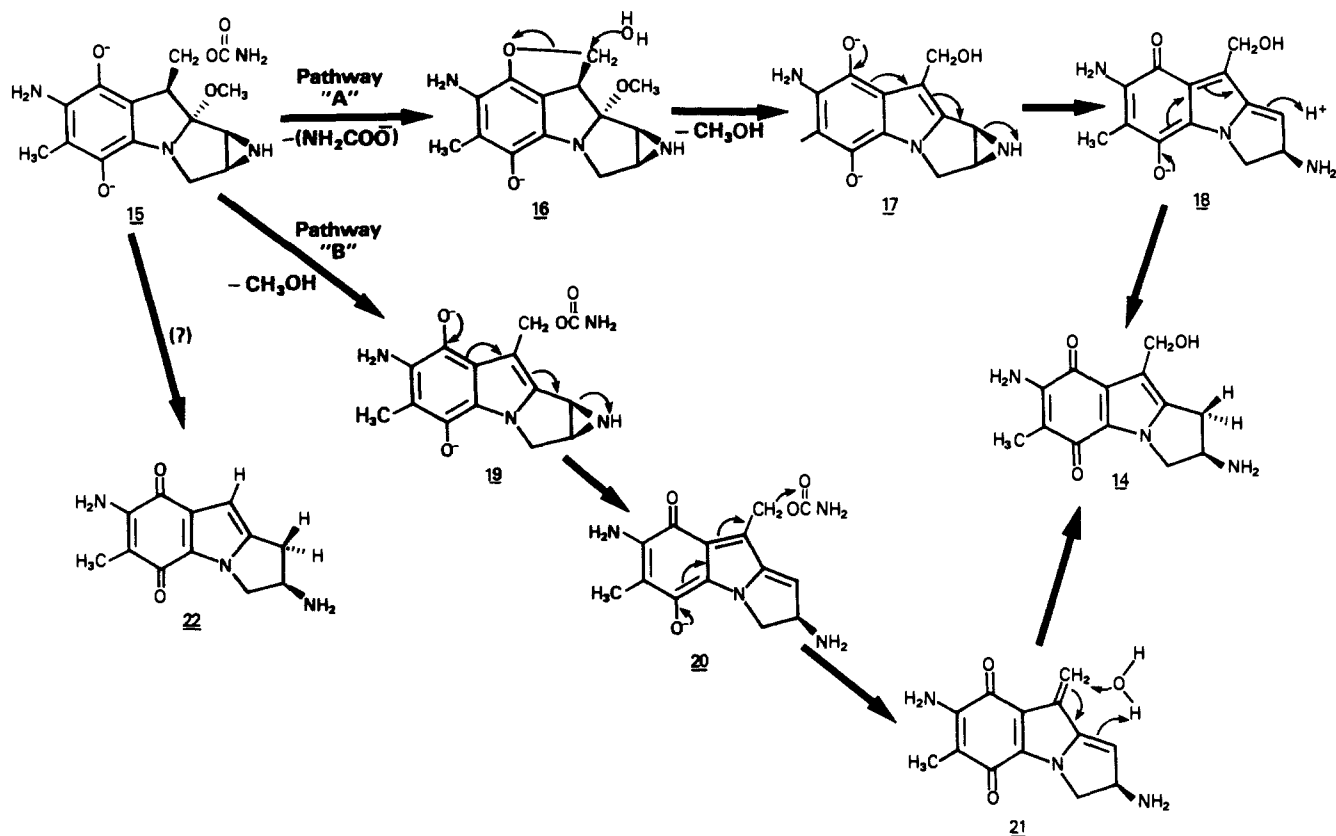


### Discussion

The lipid bilayers of cellular membranes are heterogeneous structures that present both aprotic and protic regions to entering drugs. The major bioreductive catalyst for MC activation is cytochrome P-450 reductase, a membrane-bound flavoenzyme.<sup>12-14</sup> It is certainly conceivable that MC (and other quinone-containing antibiotics) reduced in a hydrophobic catalytic site to a radical anion may be released directly into the lipid matrix surrounding the enzyme. In this aprotic environment the radical anion may have a considerable lifetime that allows its diffusion through the bilayer to distant sites where it wreaks its cytotoxic damage. In addition, the aprotic environment may favor pathways of decomposition of reduced MC that differ from protic pathways. Our study of the reductive properties of MC in the polar aprotic solvents DMF and Me<sub>2</sub>SO may thus be relevant to both the metabolic activation and mechanism of action of MC.

The MC radical anion (2) was stable in aprotic, anaerobic solutions. The addition of H<sub>2</sub>O, however, caused the rapid decomposition of this species into a complex mixture of products. Several mechanisms are proposed in Schemes I and II to explain the generation of these compounds. The polar environment af-

Scheme III



forded by the addition of water favors the loss of methanol and drives the aromatization of MC to the indoloquinone 3 (Scheme I, pathway A). Opening of the aziridine is then facilitated by delocalization of the electron density residing on  $\text{O}^8$  to generate intermediate 4A. Attack of  $\text{OH}^-$  on the positive center at C-1 leads to 5, the radical anion of the *cis*- and *trans*-hydroxymitosenes 6 and 7. Subsequent reoxidation of 5 by oxygen leads directly to 6 and 7. This pathway is more favored at basic pH (Figure 5). An alternative pathway (Scheme I, pathway B) differs from pathway A in that intermediate 4B, instead of undergoing nucleophilic attack at C-1, delocalizes the free electron at  $\text{O}^5$  to generate a carbon-centered free radical at C-1. This intermediate then abstracts an H atom to generate product 8. Pathways A and B will be in competition for the decomposition of the MC radical anion. Pathway A will be favored at more basic pH, due to increased availability of  $\text{OH}^-$  to attack C-1. Pathway B is thus favored at acidic pH, as was previously observed when 8 was generated by enzymatic reduction.<sup>12</sup> Previous reports, which studied the generation of 8 from MC following reduction by both microsomes and by  $\text{H}_2$  over  $\text{PtO}_2$ , have proposed mechanisms whereby 8 arises from the two-electron-reduced hydroquinone species.<sup>11,33</sup> Our results indicate that one-electron reduction of MC is sufficient to generate this product. It will be of interest to determine whether the remarkable stereoselective substitution of H at C-1 observed after catalytic hydrogenation<sup>33</sup> (H adds *trans* to  $\text{N}^2$ ) is maintained following one-electron electrochemical reduction.

An unusual result was the generation of 10-decarbamoyl-MC (11) and 10-decarbamoylmitosenes 12 and 13 following one-electron reduction. The leaving ability of the C-10 carbamoyl group has long been a tenet of mechanisms that explain the DNA interstrand cross-linking ability of MC.<sup>10,11,16-18</sup> Direct evidence of substitution at C-10 has come only from sodium dithionite reductions of MC in solutions with ethyl xanthate, ethyl monothiocarbonate, and thiobenzoate.<sup>36-38</sup> The loss of the carbamoyl

group to generate 11 was difficult to rationalize, since without the intermediate loss of methanol the electron density in the quinone ring is not conjugated with C-10. In Scheme II, we propose that the negative charge on  $\text{O}^8$  facilitates the loss of the C-10 carbamoyl group through anchimeric assistance. The resultant strained five-membered ring 9 is then subject to nucleophilic attack at C-10 by water to generate intermediate 10. Intermediate 10 can then decompose by pathways identical with that of MC in Scheme I to generate the *cis*- and *trans*-hydroxymitosenes 12 and 13 and compound 14 (analogous to 8). Reoxidation of 10 leads directly to 11.

When dianion 15, generated by two-electron reduction of MC, was mixed with water, only two products were formed, 14 and 22. Two pathways can be proposed to explain the formation of 14 from the dianion. Anchimeric assisted loss of the C-10 carbamoyl group by  $\text{O}^8$  leads to 16 (Scheme III, pathway A). Nucleophilic attack at C-10 by water opens the five-membered ring (as in Scheme II), and loss of methanol leads to 17. The aziridine ring is then opened by delocalization of the  $\text{O}^8$  negative charge to generate 18. Protonation of 18 at C-1 generates 14. Alternatively, as conventionally depicted, loss of methanol to generate 19 followed by delocalization of the negative charge of the dianion to generate the quinone methide 21 can be proposed (Scheme III, pathway B). Attack of water at C-10 of 21 then leads to 14. We favor pathway A as the mechanism of formation of 14 since intermediate 21 in pathway B would also be expected to produce compound 27 if attack of water were to occur at C-1 instead of C-10. The origin of the unique mitosene 22 is uncertain, and we can propose no logical mechanism to explain its origin. The complete suppression of the formation of 22 by 0.1 M phosphate is also a fascinating observation with no obvious explanation.

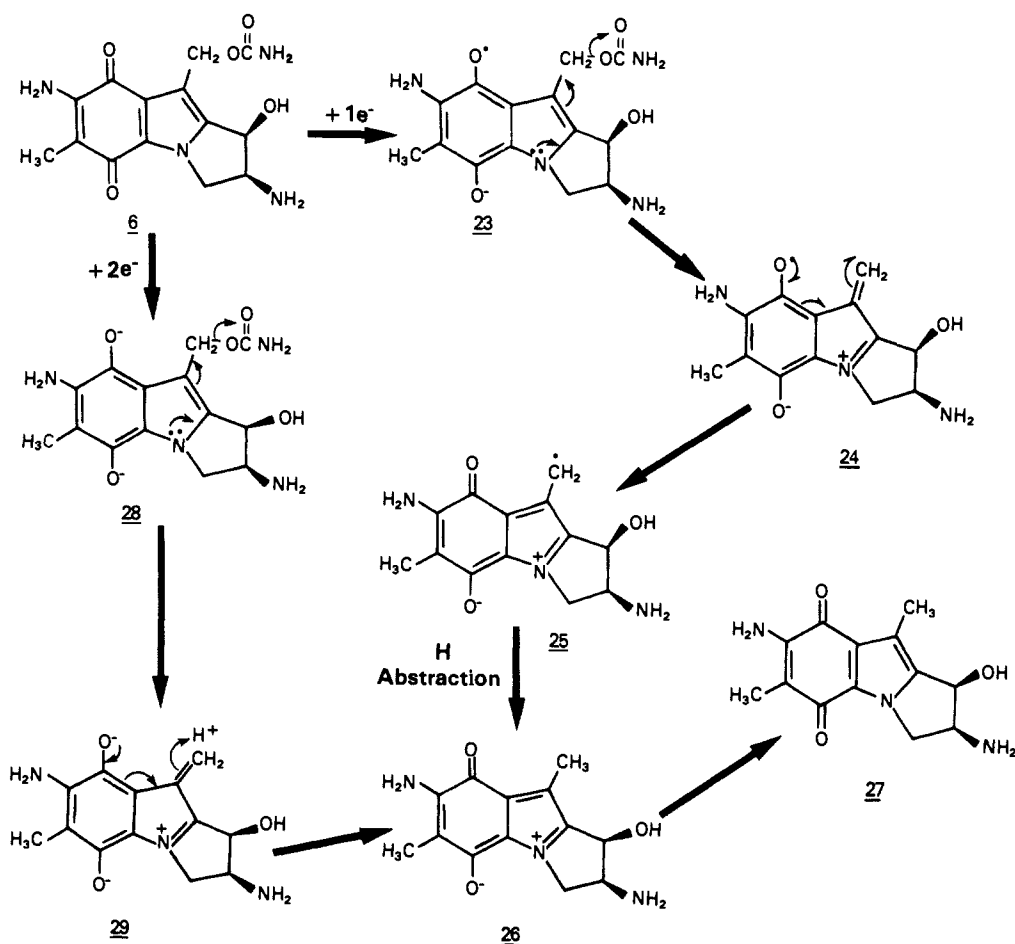
Reduction of a major mitosene metabolite of MC, 6, with either one electron or two electrons in DMF and mixture with  $\text{H}_2\text{O}$  produced only one product, 27. Decomposition pathways following one-electron and two-electron reduction are proposed in Scheme

(36) Hornemann, U.; Iguchi, K.; Keller, P. J.; Vu, H. M.; Kozlowski, J. F.; Kohn, H. *J. Org. Chem.* **1983**, *48*, 5026-5033.

(37) Bean, M.; Kohn, H. *J. Org. Chem.* **1983**, *48*, 5033-5041.

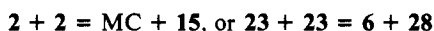
(38) Bean, M.; Kohn, H. *J. Org. Chem.* **1985**, *50*, 293-298.

Scheme IV



IV. Delocalization of the N-4 lone pair in radical-anion **23** assists the displacement of the C-10 carbamoyl group to generate intermediate **24**. This is consistent with studies on the hydrogenolysis and methanolysis of 3-indolylcarbinyl compounds.<sup>39,40</sup> Rearrangement of **24** gives the carbon-centered benzylic free radical at C-10, **25**. H abstraction by **25** leads to **26**, which is just a resonant form of **27**. Following two-electron reduction of **6**, the carbamoyl group in dianion **28** is lost in aqueous solutions by assistance from the N-4 lone pair to produce intermediate **29**. Protonation at C-10 leads to **26**, which resonates to **27**. The C-1 hydroxy substituent of **6** appears to be stable to displacement following reduction. In contrast, reduction of MC leads rapidly to displacement of the C-1 aziridinyl nitrogen to generate an intermediate reactive at C-1. This difference may be traced to relief of the aziridine ring strain in MC. This inertness of the 1-hydroxy group in **6** to displacement explains why only one product was generated since this prevented the formation of a variety of intermediates (i.e., **4**, **18**, and **20**). We have previously shown that enzymatic reduction of **6** (or **7**) also leads to one unidentified product.<sup>12</sup> This enzymatic product, however, did not cochromatograph with **27**.

It is unlikely that the products generated from the mixture of one-electron-reduced MC or **6** with H<sub>2</sub>O are partly due to a disproportionation reaction, i.e.



that could occur prior to decomposition to the products observed. Cyclic voltammetric studies show that the reduction potential for the transfer of a second electron to the MC radical anion in DMF is dependent upon the water content of the solution and does not merge with the reduction wave for the generation of MC radical anion until concentrations of 50% are reached (data not shown).

Although these studies were in solutions of 66% water, identical chromatographic profiles were obtained with 33% water. In addition the product profile generated after one-electron reduction was markedly different from that obtained after two-electron reduction with the exception of compound **14**. However, we have proposed mechanisms where **14** could be generated from both one-electron reduction (Scheme II) and two-electron reduction (Scheme III). If disproportionation was a major factor, then the one-electron product profile should have closely resembled the product profile generated following direct two-electron reduction.

The cyclic voltammetry of MC and **6** was found to be less complex in aprotic solvents than in aqueous solutions.<sup>41</sup> Both electron-transfer steps for both MC and **6** were found to be quasi-reversible. It is unlikely that the shifts of  $E_p$  and  $\Delta E_p$  with scan rate can be attributed to uncompensated  $iR$  drop. DMF and Me<sub>2</sub>SO are both polar solvents, a high concentration of electrolyte (0.1 M TEAP) was present, and low concentrations of MC and **6** were used, all of which serve to keep either the resistance or the current low. The explanation for the anodic wave at -0.710 V and the cathodic shoulder at -0.800 V that arose when the switching potential is negative enough to effect two-electron reduction is not clear. It is possible that these waves are due to adsorptive phenomena. However, since they were not observed when the switching potential was -1.125 V, they would not be due to adsorption of MC or the MC radical anion but to the MC dianion. In addition, these waves predominated as the scan rate decreased; this is the opposite of the behavior expected for an adsorptive wave. The fact that the -1.200-V anodic wave diminished and the -0.710-V anodic wave increased with slower sweep rate implies that a following chemical reaction occurred after two-electron reduction. We tested for a following chemical reaction after the -1.395-V wave (ECE mechanism) by reoxidation

(39) Leete, E. *J. Am. Chem. Soc.* **1959**, *81*, 6023-6026.

(40) Lown, J. W.; Weir, G. L. *Can. J. Chem.* **1978**, *56*, 249-257.

(41) Rao, G. M.; Begleiter, A.; Lown, J. W.; Plambeck, J. A. *J. Electrochem. Soc.* **1977**, *124*, 199-202.



of a solution of the dianion produced by the flow cell. UV-visible spectral analysis indicated that the mitosane chromophore was regenerated after exposure to molecular oxygen. In addition, two-electron reduction by hydrogenation of MC over PtO<sub>2</sub> in deaerated DMF generated a colorless solution that, upon reoxidation in air, produced solely MC as indicated by HPLC, UV-visible, and mass spectral analyses.<sup>42</sup> This is consistent with a report of the hydrogenation of porfiriomycin (*N*<sup>2</sup>-methyl-MC) in DMF that also produced no change in the parent drug.<sup>43</sup> These studies indicated that the MC radical anion and dianion were thus stable in anaerobic DMF and that their decomposition was brought about by a change in the solvolysis environment when water was added. It is possible, however, that a following chemical reaction occurred after two-electron electrochemical reduction that resulted in a new product that retained the mitosane chromophore. A likely explanation for these waves that arose when the switching potential was -1.700 V is that intermediate **16** is generated. Aprotic reoxidation of two-electron reduced solutions of MC and isolation of the product(s) permit reattachment of the carbamoyl group at C-10 instead of water as shown in Scheme III. The net result is that even though **16** is formed in situ, only intact MC will be found from these solutions, as was indeed found. Similar waves were not observed in the cyclic voltammograms of **6**. It is possible that the sp<sup>2</sup> hybridization of C-9 in intermediate **28** (Scheme IV) does not permit the distortion of the C-9, C-10 bond angle such that an intermediate analogous to **16** (Scheme III) can form for the **6** dianion. This would explain the absence of these waves for **6**.

The profile of products generated following one-electron reduction of MC is remarkably similar, although not identical, to the profile of metabolites generated following reduction of MC with flavoenzymes.<sup>12</sup> Unlike the enzymatic reduction,<sup>12</sup> one-electron electrochemical reduction did not produce 1-phosphomitosenes when the radical anion was mixed with phosphate buffers. This effect may be due to the presence of high concentrations of DMF that, through either dielectric constant or solvation effects, make the phosphate ion a weaker nucleophile than in water alone. In addition to similar product profiles obtained

after one-electron and enzymatic activation, the pH dependence of these profiles follow the same trend.<sup>12</sup> Two-electron reduction in aprotic solvents dictates the formation of products different from those of both one-electron reduction in aprotic solvents and from enzyme-mediated reductions of MC. Our data provide compelling evidence that one-electron reduction of MC is sufficient to activate this molecule to alkylating intermediates and, furthermore, that this is the major bioreductive mode of metabolism. Two-electron reductions need not be invoked to account for the alkylating properties of this drug.

None of the intermediates that we have proposed to account for the products found from one-electron-reduction possess bifunctional electrophilic sites. The data imply that the DNA interstrand cross-linking may occur after two distinct bioreductive steps. The first one-electron bioreductive step generates a monofunctionally bound mitosene adduct on DNA. This adduct may be available to nuclear flavoenzymes such as cytochrome P-450 reductase for a subsequent one-electron bioreductive step to generate an intermediate analogous to **23**. This bound intermediate can then either lose its C-10 carbamate to generate an electrophilic site that cross-links the DNA or transfer its electron to molecular oxygen and produce a cascade of reactive oxygen species in close proximity to DNA.<sup>18,22</sup> The inertness of the 1-hydroxy substituent in **6** after reduction supports the possibility of this sequence of events. Also in support of this mechanism is our observation that **6** and **7** (and 1-phosphomitosenes) can be substrates for NADPH cytochrome P-450 reductase and xanthine oxidase and are metabolized to unknown products following reduction by these enzymes.<sup>12</sup> A mitosene C-1-guanine-O<sup>6</sup> bond is thus likely to be stable to subsequent bioreduction and to possess the potential for generating a second electrophilic site (through loss of the C-10 carbamate) that cross-links DNA.

**Acknowledgment.** We thank Constance J. Glover for skilled technical assistance and Dr. Robert J. Highet for providing the NMR spectra. This work was supported in part by Grant CA 33697 from the National Cancer Institute (to S.-s.P.).

**Supplementary Material Available:** A listing of mass spectral fragmentation assignments, a description of flow cell construction, and Figures 6-8 giving HPLC profiles, EI mass spectra, and a diagram of the flow cell, respectively (5 pages). Ordering information is given on any current masthead page.

(42) Andrews, P. A., unpublished observations.

(43) Patrick, J. B.; Williams, R. P.; Meyer, W. E.; Fulmor, W.; Cosulich, D. B.; Broschard, R. W.; Webb, J. S. *J. Am. Chem. Soc.* **1964**, *86*, 1889-1890.